

# Membrane-Surface Anchoring of Charged Diacylglycerol-Lactones Correlates with Biological Activities

Or Raifman,<sup>[a]</sup> Sofiya Kolusheva,<sup>[a]</sup> Said El Kazzouli,<sup>[b]</sup> Dina M. Sigano,<sup>[b]</sup> Noemi Kedei,<sup>[c]</sup> Nancy E. Lewin,<sup>[c]</sup> Ruben Lopez-Nicolas,<sup>[d]</sup> Ana Ortiz-Espin,<sup>[d]</sup> Juan C. Gomez-Fernandez,<sup>[d]</sup> Peter M. Blumberg,<sup>[c]</sup> Victor E. Marquez,<sup>\*,[b]</sup> Senena Corbalan-Garcia,<sup>\*,[d]</sup> and Raz Jelinek<sup>\*,[a]</sup>

Synthetic diacylglycerol-lactones (DAG-lactones) are effective modulators of critical cellular signaling pathways, downstream of the lipophilic second messenger diacylglycerol, that activate a host of protein kinase C (PKC) isozymes and other nonkinase proteins that share similar C1 membrane-targeting domains with PKC. A fundamental determinant of the biological activity of these amphiphilic molecules is the nature of their interactions with cellular membranes. This study examines the biological properties of charged DAG-lactones exhibiting different alkyl groups attached to the heterocyclic nitrogen of an  $\alpha$ -pyridylalkylidene chain, and particularly the relationship between membrane interactions of the substituted DAG-lactones and

their respective biological activities. Our results suggest that bilayer interface localization of the *N*-alkyl chain in the R<sup>2</sup> position of the DAG-lactones inhibits translocation of PKC isoenzymes onto the cellular membrane. However, the orientation of a branched alkyl chain at the bilayer surface facilitates PKC binding and translocation. This investigation emphasizes that bilayer localization of the aromatic side residues of positively charged DAG-lactone derivatives play a central role in determining biological activity, and that this factor contributes to the diversity of biological actions of these synthetic biomimetic ligands.

## Introduction

The lipophilic second messenger *sn*-1,2-diacylglycerol (DAG) is released in situ from membrane phosphatidylinositol 4,5-bisphosphate through the action of phospholipase C in response to the occupancy of a wide range of G protein-coupled receptors and receptor tyrosine kinases.<sup>[1]</sup> The other hydrolysis product, inositol-1,4,5-triphosphate (IP<sub>3</sub>) triggers in turn the release of calcium from intracellular stores. The released Ca<sup>2+</sup> ions promote a weak and reversible association of the classical protein kinase C (PKC) isoforms with the inner leaflet of the membrane, after which the PKC penetrates further into the membrane by its interaction with DAG. This process is accompanied by the folding out of an N-terminal pseudosubstrate region, which allows access of a myriad of substrates to the binding site of the enzyme.

As a second messenger, DAG mediates the action of numerous growth factors, hormones and cytokines by activating members of the PKC family of enzymes, as well as several other families of signaling proteins, for example, RasGRPs and chimaerins, that share with PKC the C1 domain as a DAG-recognition motif. Many of these signaling pathways feature prominently in the development and properties of cancer cells<sup>[2,3]</sup> and, in consequence, PKC isozymes are being actively pursued as therapeutic targets for cancer.<sup>[4]</sup> The majority of C1 binding ligands that are utilized are structurally rigid and complex natural products, such as the prototypical phorbol esters and the bryostatins.<sup>[5]</sup> These compounds bind to their C1 receptors with nanomolar affinities and are more than three orders of magnitude more potent than the very flexible, natural DAG agonists.

During the past several years we have developed a family of conformationally constrained DAG analogues, known as DAG-lactones, which were designed to overcome this spread in potency between the natural product ligands and DAG.<sup>[6]</sup> The generation of the prototypical DAG-lactone template (I) is conceptually simple and involves the joining of the *sn*-2-*O*-acyl moiety of DAG to the glycerol backbone with an additional carbon atom to complete a five-membered ring (Scheme 1).

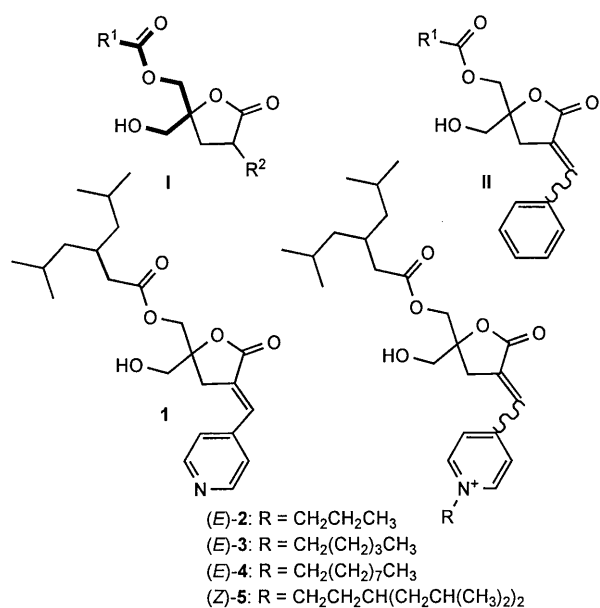
[a] O. Raifman, Dr. S. Kolusheva, Prof. R. Jelinek  
Department of Chemistry, Ben Gurion University  
Beer Sheva 84105 (Israel)  
Fax: (+972) 8647-2943  
E-mail: razj@bgu.ac.il

[b] Dr. S. El Kazzouli, Dr. D. M. Sigano, Dr. V. E. Marquez  
Laboratory of Medicinal Chemistry, Center for Cancer Research  
National Cancer Institute at Frederick, National Institutes of Health  
Frederick, MD 21702 (USA)  
Fax: (+1) 301-846-6033  
E-mail: marquezv@dc37a.nci.nih.gov

[c] Dr. N. Kedei, Dr. N. E. Lewin, Dr. P. M. Blumberg  
Laboratory of Cancer Biology and Genetics  
Center for Cancer Research, National Cancer Institute  
Bethesda, MD 20892 (USA)

[d] R. Lopez-Nicolas, A. Ortiz-Espin, J. C. Gomez-Fernandez,  
Prof. S. Corbalan-Garcia  
Department of Biochemistry and Molecular Biology-A  
Veterinary School, University of Murcia, 30100 Murcia (Spain)  
Fax: (+34) 968-364147  
E-mail: senena@um.es

 Supporting information for this article is available on the WWW under <http://dx.doi.org/10.1002/cbic.201000343>.



**Scheme 1.** I) Structure of a DAG-lactone prototype with the embedded DAG backbone shown with heavier lines. II) Structure of a prototype DAG-lactone with an  $\alpha$ -arylalkylidene chain. The lower panel shows the structures of compounds 1–5.

Some of the most interesting DAG-lactone templates that we have studied are those with an  $\alpha$ -arylalkylidene chain (II). These compounds seem to bind to PKC with the acyl chain (R<sup>1</sup>) oriented toward the interior of the membrane and the  $\alpha$ -arylalkylidene chain directed to the surface of the C1 domain adjacent to the lipid interface.<sup>[7]</sup>

Because electrostatic interactions are important for the initial membrane-binding process of PKC, particularly at the lipid-bilayer interface, we decided to exploit the role of electrostatic attraction by converting the aryl group in II to a substituted pyridine ring. We reasoned that the pyridine ring could bear several alkyl groups of various sizes to generate a series of *N*-alkylpyridinium chains that could bind to negatively charged phospholipids or engage in cation- $\pi$  interactions between the positively charged  $\pi$  system and aromatic rings of certain amino acids in the C1 domain, such as tryptophan, that ought to be stabilized through van der Waals and  $\pi$ - $\pi$  stacking interactions.<sup>[8]</sup>

The specific charged compounds that were designed (2–5, Scheme 1) have different  $\alpha$ -(4-*N*-alkylpyridinium)alkylidene side chains, which are derived from the parent, neutral DAG-lactone 1 by simple alkylation. Although the stereochemistry around the double bond could be either *E* or *Z*, all of the compounds with the exception of 5 favored the *E* stereochemistry. In all the DAG-lactones (1–5) the most efficient, branched acyl chain known to enhance membrane penetration was chosen,<sup>[6]</sup> and at the other end of the molecule the  $\alpha$ -(4-*N*-alkylpyridinium)alkylidene side chains were expected to interact near the surface of the C1 domain adjacent to the lipid interface.

Here, we investigated the translocation properties, PKC binding, and lipid bilayer interactions of DAG-lactones 1–5 (Scheme 1). These ligands are shown to induce different patterns and kinetic profiles for translocation of PKC isoforms to

membranes, and this study aims to examine whether the pattern of membrane association might account for the biological differences. Application of biophysical techniques, including fluorescence quenching<sup>[9]</sup> and differential scanning calorimetry (DSC),<sup>[10]</sup> underscore the prominent contribution of the alkyl residue in the aromatic unit (position R<sup>2</sup>) to the biological activities of the DAG-lactone. In particular, our data point to a relationship between bilayer surface localization and disruption by the alkyl residues and binding/translocation of the PKC isoforms. Overall, the results expand our understanding of the molecular parameters effecting PKC translocation to membranes by synthetic DAG-lactones.

## Results

### Membrane translocation

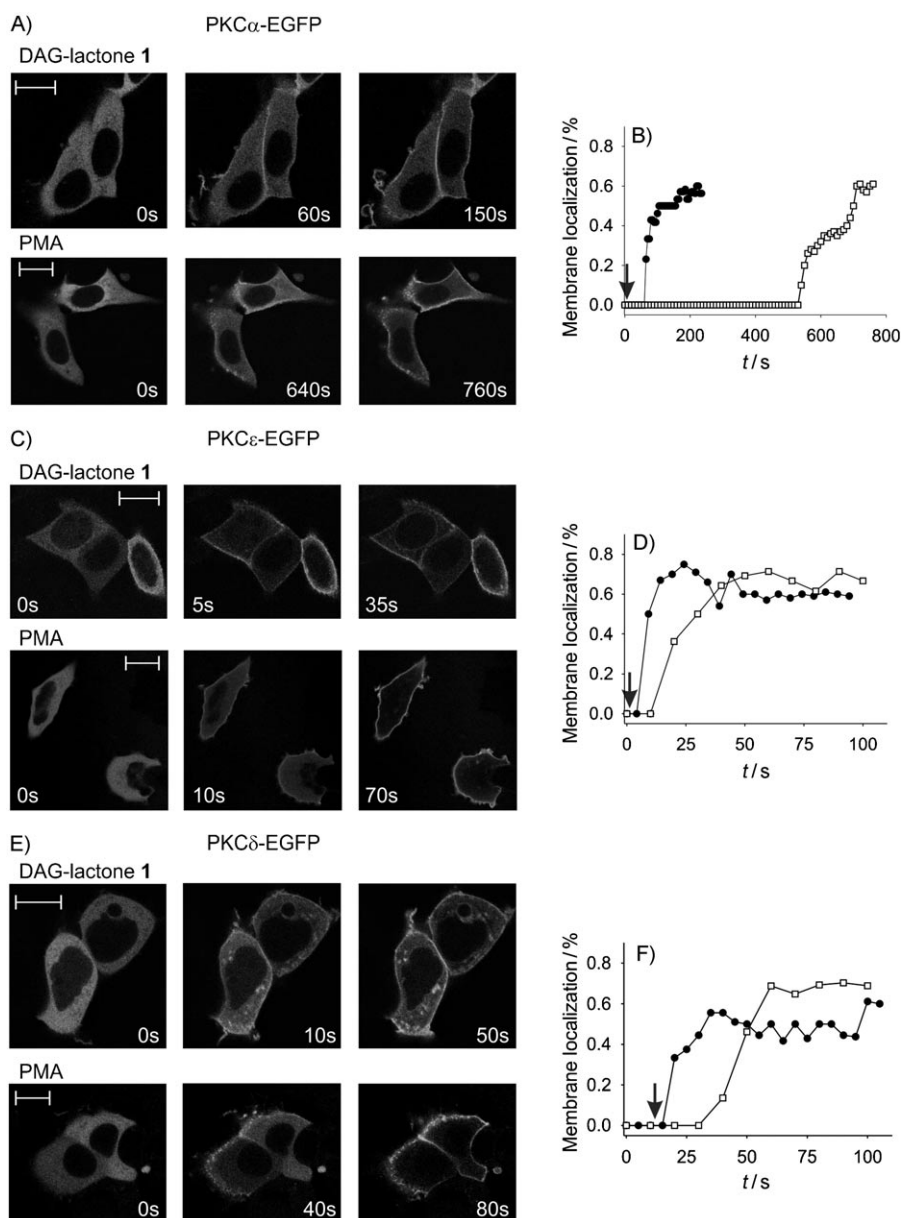
Analysis of the translocation of three PKC isoforms induced by DAG-lactones 1–5 showed pronounced differences among the compounds (Figure 1 and Table 1). The translocation analysis utilized MCF-7 cells that were transiently transfected with the fluorescent constructs PKC $\alpha$ -EGFP (representative of classical isoenzymes), PKC $\epsilon$ -EGFP or PKC $\delta$ -ECFP (representative of each of the two subgroups of novel PKCs). Also presented in Figure 1 and Table 1 is a comparison with the translocation induced by phorbol 12-myristate 13-acetate (PMA, the standard derivative used to characterize responses of PKC to phorbol esters or other ligands targeted to the C1 domain).

Figure 1 shows the DAG-lactone 1 induced plasma membrane localization of all three isoenzymes tested. The percentage of protein localized in the plasma membrane ( $R_{\max}$ ) was similar for the three isoenzymes (Table 1), although the membrane distribution was heterogeneous and the three proteins appeared localized in distinct areas of the plasma membrane. In addition, Figure 1 indicates that 1 gave rise to localization of PKC $\delta$ -ECFP in vesicles distributed through the cytosol (Figure 1E) suggesting that the protein and/or lipid composition of these vesicles influenced the targeting effect of the DAG-lactone as compared to PMA in the case of this isoenzyme.

**Table 1.** Plasma membrane translocation parameters calculated for the different PKC isoenzymes in MCF-7 cells stimulated with DAG-lactones.

DAG-lactone	Isoenzyme	$R_{\max}$ [a] [%]	$t_{1/2}$ [b] [s]
1	PKC $\alpha$	0.62 ± 0.04	62 ± 13
	PKC $\epsilon$	0.6 ± 0.16	3.5 ± 1.7
	PKC $\delta$	0.56 ± 0.12	15 ± 4.3
2–4	PKC $\alpha$	no effect	no effect
	PKC $\epsilon$	no effect	no effect
	PKC $\delta$	no effect	no effect
5	PKC $\alpha$	no effect	no effect
	PKC $\epsilon$	0.77 ± 0.1	21 ± 5
	PKC $\delta$	0.65 ± 0.07	24 ± 9
PMA	PKC $\alpha$	0.64 ± 0.08	547 ± 192
	PKC $\epsilon$	0.68 ± 0.08	31 ± 18
	PKC $\delta$	0.72 ± 0.06	47 ± 22

[a] Maximal percentage of protein localized in the plasma membrane.  
 [b] Half-time of plasma membrane localization.



**Figure 1.** Effect of DAG-lactone 1 on the plasma membrane localization of PKC isoenzymes. Confocal images of MCF-7 cells expressing: A) PKC $\alpha$ -EGFP, C) PKC $\epsilon$ -EGFP, or E) PKC $\delta$ -EGFP stimulated with 40  $\mu$ M DAG-lactone 1 (upper panels) or 40  $\mu$ M PMA (lower panels). Time in seconds after stimulation is indicated in each micrograph. The protein localization was measured by a line profile (pixel density) traced in each frame as indicated in the Experimental Section. The resulting net change in: B) PKC $\alpha$ -EGFP, D) PKC $\epsilon$ -EGFP, or F) PKC $\delta$ -EGFP plasma membrane localization upon DAG-lactone (●) and PMA (□) stimulations is expressed as the  $(I_{mb} - I_{cyt})/I_{mb}$  ratio (%) and is represented versus time. The arrow indicates the stimulation time;  $R_{max}$  and  $t_{1/2}$  parameters were calculated graphically.<sup>[18]</sup> The profiles are representative of the results obtained in the cells analyzed ( $n = 16$  for both DAG-lactone and PMA for PKC $\alpha$ -EGFP;  $n = 12$  and 10 for DAG-lactone and PMA, respectively, for PKC $\epsilon$ -EGFP;  $n = 13$  and 12 for DAG-lactone and PMA, respectively, for PKC $\delta$ -EGFP). The scale bars correspond to 12  $\mu$ m.

Comparison of the half-times of plasma membrane localization ( $t_{1/2}$ , Table 1) demonstrates that 1 effected PKC $\epsilon$ -EGFP translocation to the plasma membrane significantly faster as compared to PKC $\delta$ -EGFP followed by PKC $\alpha$ -EGFP, suggesting that PKC $\epsilon$ -EGFP exhibits higher affinity for 1 compared to PKC $\delta$ -EGFP and PKC $\alpha$ -EGFP. Figure 1 and Table 1 further show that 1 induced significantly faster translocation to the plasma membrane than PMA with all PKC isoforms; this is consistent with more rapid penetration. The additions of nonbranched *N*-

(*n*-alkylpyridinium) chains of different lengths in the R<sup>2</sup> position of 1 completely eliminated the translocation capabilities when these derivatives were added to MCF-7 cells transfected with the different isoenzymes (Table 1). This result highlights the biological significance of the positive charge generated by the presence of *N*-(*n*-alkylpyridinium) residues, and the following experimental analysis is designed to elucidate the effects of the side chains.

The DAG-lactone 5, which still bears a positive charge, displays a branched alkyl chain in the R<sup>2</sup> position instead of a linear *n*-alkyl chain. Remarkably, this structural change facilitated translocation of the novel PKCs (PKC $\epsilon$ -EGFP and PKC $\delta$ -EGFP) from the cytosol to the plasma membrane at very similar rates (Figure 2A–D and Table 1), although the percentage of PKC $\epsilon$ -EGFP localized at the plasma membrane was slightly higher than that of PKC $\delta$ -EGFP (Table 1). This DAG-lactone derivative also induced the localization of PKC $\delta$ -EGFP in vesicles distributed through the cytosol (Figure 2B). This effect was not observed when the cells were stimulated with PMA, suggesting that the localization of the enzyme in vesicles is directly related to effects of the DAG-lactones.

### Dissociation constants

The binding potencies of the DAG-lactones were evaluated in vitro by competition of binding

of [<sup>3</sup>H]phorbol 12,13-dibutyrate to PKC in the presence of 100  $\mu$ g mL<sup>-1</sup> phosphatidylserine (Table 2). In parallel with the findings from the cellular translocation studies, DAG-lactone 5, possessing the branched alkyl chain in the R<sup>2</sup> position, showed similar binding potency to the uncharged DAG-lactone 1. In contrast, the three DAG-lactones 2–4, which possessed nonbranched *N*-(*n*-alkylpyridinium) chains together with a positive charge, were approximately an order of magnitude less potent.

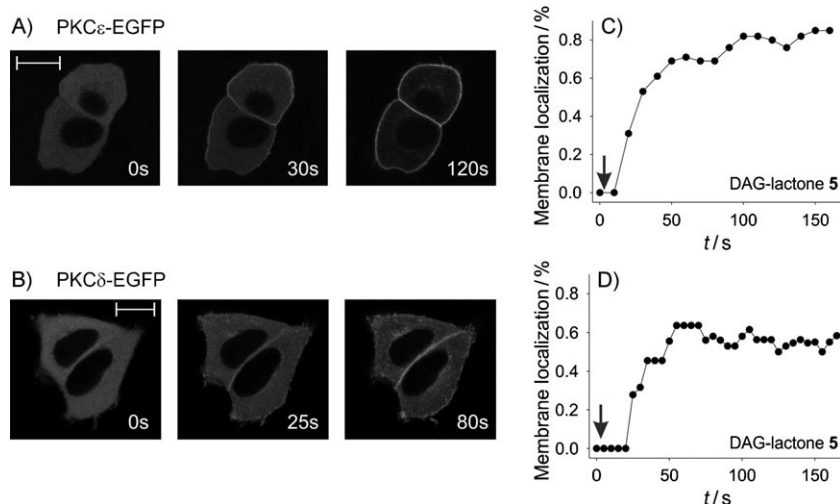


**Figure 2.** Effect of DAG-lactone 5 on the plasma membrane localization of PKC isoenzymes. Confocal images of MCF-7 cells expressing: A) PKC $\epsilon$ -EGFP, or B) PKC $\delta$ -EGFP stimulated with 40  $\mu\text{M}$  DAG-lactone 5. Time in seconds after stimulation is indicated in each micrograph. The scale bars correspond to 12  $\mu\text{m}$ . C), D) The percentage of protein localization was measured by a line profile (pixel density) traced in each frame as indicated in the Experimental Section. The resulting net change in PKC $\epsilon$ -EGFP or PKC $\delta$ -EGFP plasma membrane localization upon DAG-lactone (●) stimulation is expressed as the  $(I_{\text{mb}} - I_{\text{cyt}})/I_{\text{mb}}$  ratio (%) and is represented versus time. The arrow indicates the stimulation time;  $R_{\text{max}}$  and  $t_{1/2}$  parameters were calculated graphically.<sup>[18]</sup> The profiles are representative of the results obtained in the cells analyzed ( $n = 12$  and 10 for PKC $\epsilon$ -EGFP or PKC $\delta$ -EGFP, respectively).

Compound	$K_i$ [nM] <sup>[a]</sup>	Compound	$K_i$ [nM] <sup>[a]</sup>
DAG-lactone 1	88.5 $\pm$ 3.3	DAG-lactone 2	1800 $\pm$ 150
DAG-lactone 3	1340 $\pm$ 240	DAG-lactone 4	1210 $\pm$ 41
DAG-lactone 5	188 $\pm$ 17		

[a] Values are the mean  $\pm$  SEM of triplicate experiments. Binding potencies were determined by competition of [ $^3\text{H}$ ]PDBu binding and represent the inhibitor dissociation constant,  $K_i$ .

### Biophysical analyses

The membrane translocation and binding analyses summarized in Figures 1 and 2 and Tables 1 and 2 point to significant differences in biological activities of the DAG-lactones 1–5. To evaluate the relationships between the biological properties of the compounds and their association with the cell membrane we applied several biophysical techniques for investigating interactions of 1–5 with lipid vesicles (Figures 3 and 4). In particular, the biophysical experiments were designed to assess the contributions of the positive charge and the alkyl residues in position R<sup>2</sup> to membrane interactions and localization of the compounds.

To probe the extent of the localization of DAG-lactones 1–5 at the bilayer/water interface we carried out fluorescence quenching experiments utilizing DMPC vesicles into which the fluorescent probe NBD-PE was incorporated<sup>[9]</sup> (Figure 3). The NBD dye in lipid vesicles is embedded close to the bilayer interface, thus providing a useful marker for surface interactions of membrane-active compounds. The experiments summarized in Figure 3 depicts the modulation of the fluorescence quench-

ing of NBD by water-dissolved sodium dithionite following preincubation of the vesicles with the DAG-lactones, providing a measure of bilayer interactions of the compounds.<sup>[9]</sup>

Figure 3 demonstrates that incubation of the NBD-PE-DMPC vesicles with the DAG-lactones yielded significant changes in the rate of dithionite-induced fluorescence quenching of the bilayer-embedded dye. Importantly, while 1 did not effect the fluorescence quenching rate of NBD (compared to the control vesicles), all the other charged DAG-lactones examined yielded faster quenching compared with vesicles that were not preincubated with the DAG-lactones prior to addition of sodium dithionite. Faster quenching of the

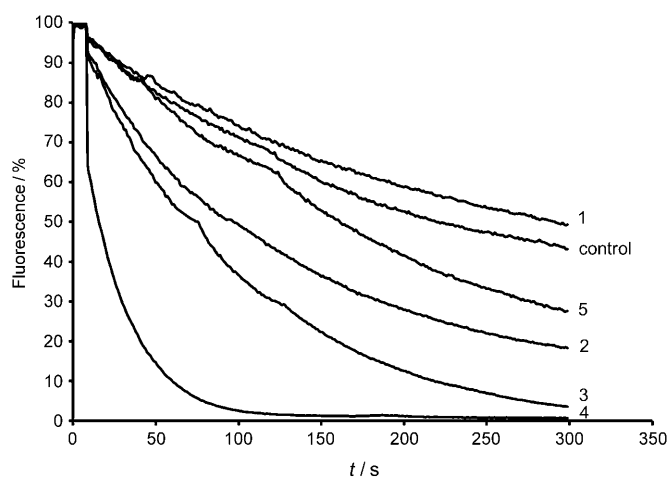


**Figure 3.** Fluorescence quenching. Fluorescence intensities of NBD-PE dye embedded within DMPC vesicles following preincubation with DAG-lactones 1–5. Initial fluorescence (at  $t = 0$ , upon addition of sodium thionite) is defined as 100%.

fluorescent dye is indicative of disruption of the bilayer head-group region, which consequently results in greater exposure of the dye to the water-soluble dithionite.<sup>[9]</sup>

The differences in the quenching rates of NBD among the DAG-lactones 2–5, apparent in Figure 3, point to distinct modes of bilayer binding by the compounds. Specifically, preincubation of 4 with the NBD-PE-DMPC vesicles yielded pronounced quenching significantly faster than all other compounds (Figure 3). This result indicates substantial disruption of the lipid bilayer surface by 4. Figure 3 also shows that 2 and 3 enhanced the dithionite-induced quenching rate of NBD, although to a lesser extent compared to 4. These results are still

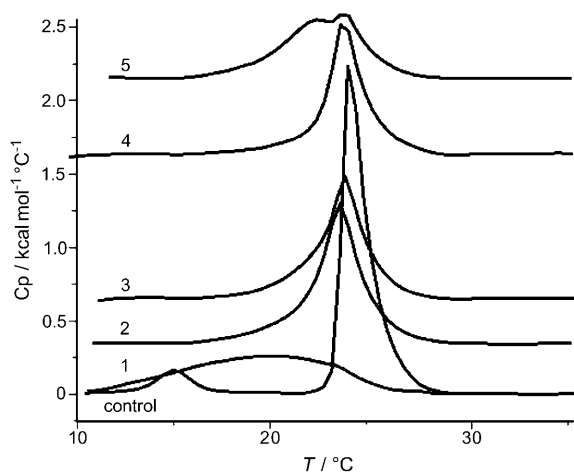


**Figure 4.** DSC thermograms. Spectra were acquired following incubation of DAG-lactones 1–5 with DMPC multilamellar vesicles.

indicative of a relatively pronounced bilayer surface localization of 2 and 3. DAG-lactone 5, on the other hand, moderately increased the fluorescence quenching rate, suggesting that bilayer interface interactions of this DAG-lactone were not as significant as those of 2, 3, and 4.

Figure 3 points to different degrees of localization and perturbation of the bilayer headgroup region. To further probe the interactions of the DAG-lactones with lipid bilayers and their effects on the bilayer properties we carried out DSC measurements (Figure 4). DSC allows examination of the cooperative properties of lipid bilayers, and the modification of these properties by interactions of membrane active molecules.<sup>[10]</sup>

The DSC thermograms in Figure 4 and corresponding spectral parameters in Table 3 indicate that DAG-lactones 1–5 exerted different effects on the lipid bilayers. Specifically, 2, 3, and 4 gave rise to a very similar narrow Gaussian signal for DMPC at around 22 °C (Figure 4). Furthermore, the DSC parameters ( $T_m$  and  $t_{1/2}$ ) corresponding to the vesicles incubated with DAG-lactones 2–4, shown in Table 3, appear close to the values derived from the thermogram of the control vesicles (Table 3). These results are consistent with the fluorescence quenching data in Figure 3, which points to prevalent bilayer–surface interactions by 2–4; localization of the DAG-lactones in the region of the lipid headgroups is indeed hardly expected to effect the lipid bilayer thermal transitions, which depend primarily on the dynamics of the phospholipids' alkyl chains.<sup>[11]</sup>

Table 3. DSC parameters obtained from thermograms.					
DAG-lactone	$T_m$ <sup>[a]</sup>	$\Delta H$ <sup>[b]</sup>	DAG-lactone	$T_m$ <sup>[a]</sup>	$\Delta H$ <sup>[b]</sup>
control <sup>[c]</sup>	24.1	3480	1	19.4	2600
2	23.4	2690	3	23.6	2250
4	23.7	2070	5	22.6	2200

[a] Maximum of DSC spectrum (weighted average, °C). [b] Enthalpy change (cal mole<sup>-1</sup>). [c] No addition.

In contrast to the minor modulation of the DMPC thermogram by DAG-lactones 2–4, Figure 4 demonstrates that 1 and 5 give rise to significant spectral changes. In particular, the appearance of an extremely broad peak following incubation of the DMPC vesicles with 1 demonstrates that the impact of this DAG-lactone upon the cooperative properties of the bilayer was substantial. The broad thermal transition induced by 1 indicates that this derivative is closely incorporated within the lipid bilayer, strongly modulating lipid interdigitation.

The DSC trace of 5 also displays a significant difference compared to DAG-lactones 2–4 (Figure 4). Interestingly, the DSC thermogram of 5 appears to show two populations of the molecule. One population, giving rise to a relatively narrow transition exhibiting  $T_m$  of 23.6 °C (Table 3), most likely corresponds to the DAG-lactone in a bilayer interface orientation, similar to the localization of 2–4. However, a second, broader peak ( $t_{1/2} = 3.3$  °C) in the DSC thermogram exhibiting  $T_m$  of 21.6 °C most likely corresponds to a subpopulation of 5 that is embedded deeper within the lipid bilayer, consequently interfering with the thermal transition of the phospholipids in a similar manner to 1. This interpretation is also consistent with the NBD quenching result of 5 (Figure 3), which indicates a low degree of bilayer surface disruption by this ligand.

## Discussion

This study is part of a comprehensive effort in our laboratories aimed at elucidating the relationships between membrane anchoring of synthetic DAG-lactones and the cellular activities of these ligands.<sup>[12,13]</sup> The data presented here indicate that the biological properties of DAG-lactones 1–5 are indeed closely dependent upon the modes of membrane anchoring of the molecules, particularly the extent of their binding and localization at the bilayer/water interface.

Our results demonstrate that the parent DAG-lactone 1, which does not carry a positive charge, inserts into the hydrophobic core of the lipid bilayer rather than accumulating at the membrane surface. This characteristic most likely contributes to the effective translocation capabilities of this ligand in the biological experiments. In contrast to 1, which efficiently inserts into the membrane bilayer, DAG-lactones 2–4 appear specifically localized at the bilayer/water interface (Figure 3 and 4). This feature is most likely associated with the extended *n*-alkyl side residues in the R<sup>2</sup> position, which do not shield the positive amine, thereby retaining its electrostatic attraction to the phosphate moieties of the phospholipid headgroups. The pronounced bilayer surface interactions of DAG-lactones 2–4 is the probable factor accounting for the absence of PKC translocation with these ligands. These results fit with the determination of ligand binding affinities for PKC. Since the role of ligand binding to the C1 domain of PKC is to facilitate the insertion of the C1 domain into the lipid bilayer, driving translocation, those ligands that do not insert into and disrupt the bilayer structure are less effective at promoting this insertion, although other factors will also play a role.

DAG-lactone 5 was shown to induce translocation of PKC $\delta$  and PKC $\epsilon$ , but not PKC $\alpha$  (Figure 1, Table 1). This observation

might be related to the intermediate status of lipid bilayer interactions of this ligand exhibiting lesser bilayer interface interactions compared to **2–4**, and partial insertion into the lipid bilayer (Figures 3 and 4). In particular, the DSC data in Figure 4 suggest that two populations of **5** exist in relation to membrane interactions; deeper penetration of a subpopulation of **5** is most likely responsible for inducing membrane translocation of the PKCs. The biophysical data indicate that the branched alkyl chain and the *Z* stereochemistry of the double bond of **5** are the structural determinants promoting internalization of the side residue beyond the bilayer surface through possible shielding of the positive charge, thus facilitating the biological functionality of the ligand.

Additional explanation for the differential effect on plasma membrane translocation among the different PKC isoenzymes might be also found in the small variations in the surface charges exhibited by the C1 domains at the rim of the DAG-lactone binding cleft. Figure 5 depicts an example in which solvent-accessible surfaces have been modeled into the 3D structures of the C1B domains of PKC $\alpha$  and PKC $\delta$ , respectively. It is apparent in the model shown in Figure 5 that the surface and the rim of the top region of the PKC $\alpha$  molecule, which includes the DAG-lactone interacting site, are more hydrophobic than in PKC $\delta$ . Note that the C1B domain of PKC $\delta$  exhibits a positive charge corresponding to Lys256, which is conserved in PKC $\epsilon$  (Arg267) but not in the C1B domain of PKC $\alpha$  (His128; Figure 5). Taking also into account the deeper membrane dis-

position of DAG-lactone **5** compared to DAG-lactones **2–4**, these positively charged residues in the C1 domain of PKC $\delta$  and PKC $\epsilon$ , which might initially contribute to the approach of the compounds to the plasma membrane interface in a more favorable orientation than PKC $\alpha$ , thus enabling the docking of the lactone ring in a second step.

The divergent behavior of compounds **1–5** is particularly intriguing. Combinatorial libraries of DAG-lactones indicate that marked differences in biological response could be generated from modest structural variations in the hydrophobic domains of the DAG-lactones.<sup>[7]</sup> The probable interpretation of those observations was that the differential effects reflected changes in the pattern of association of the various PKC isoforms and other C1 domains containing effector proteins with membrane microdomains. The present findings indicate that the combination of positive charge, which should be selective for negatively charged membrane regions, together with appropriate variation in the hydrophobic moieties incorporated into the structure, can likewise have profound effects on the pattern of interaction with membranes. Although not examined in the present studies, such positively charged ligands should also be influenced in their selectivity by differences in membrane potential or local pH, whether with cells or cellular organelles, such as mitochondria or lysosomes. We conclude that incorporation of charged moieties into DAG-lactones affords a promising strategy for generation of diversity within this class of ligands.

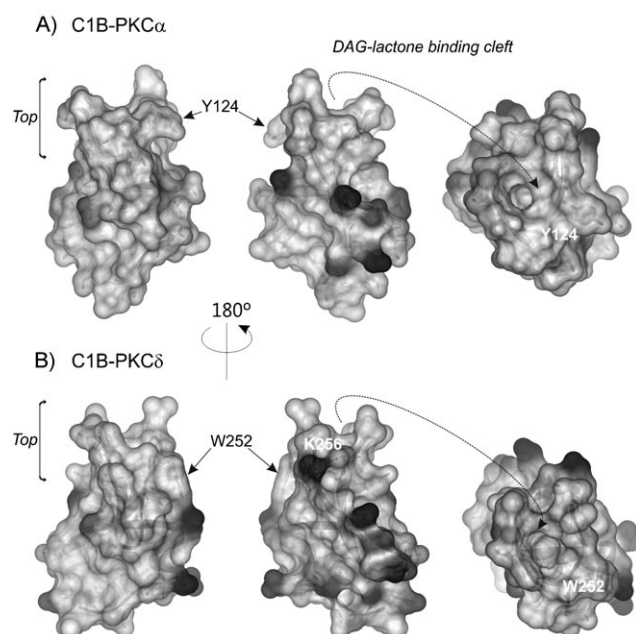


**Figure 5.** Solvent accessible surface of the C1B domain of: A) PKC $\alpha$ , and B) PKC $\delta$  in the absence of ligands. The structures were calculated by using DSVisualizer 2.0 with a probe radius of 1.4 Å. Positively and negatively charged regions are shown in dark and light gray, respectively, while the hydrophobic surface is represented in white. Amino acid residues of reference have been labeled to help orientate the molecules. The molecules on the left correspond to a front view with critical W or Y residues labeled. The molecules on the center correspond to the back view, and those in the right correspond to a top view showing the DAG-lactone binding cleft.

## Conclusions

In this study we examined the relationship between membrane interactions and biological activities of charged DAG-lactones exhibiting different alkyl groups attached to the heterocyclic nitrogen of an  $\alpha$ -pyridylalkylidene chain. The experimental data indicate that the extent of bilayer insertion of the non-branched, *N*-(*n*-alkylpyridinium) chains of the positively charged DAG-lactones intimately and significantly effect the translocation capabilities of the molecules. We observed that deeper insertion of the biomimetic DAG-lactone ligands into the membrane is essential for facilitating recognition of the ligands by PKC—a prerequisite for inducing translocation. In contrast, anchoring of the DAG-lactones displaying positively charged *N*-(*n*-alkylpyridinium) linear chains on the membrane surface interferes with their recognition and accessibility to the PKC enzymes, eliminating translocation. Overall, our analysis underscores the significance of membrane anchoring and insertion for the biological action of the DAG-lactone derivatives.

## Experimental Section

**Materials:** 1,2-Dimyristoyl-*sn*-glycero-3-phosphocholine (DMPC) was purchased from Avanti (Alabaster, AL, USA). Sodium dithionite (Na<sub>2</sub>O<sub>4</sub>S<sub>2</sub>) and tris(hydroxymethyl)aminomethane (TRIZMA base buffer, C<sub>4</sub>H<sub>11</sub>NO<sub>3</sub>) were purchased from Sigma. The fluorescent dye *N*-(7-nitrobenz-2-oxa-1,3-diazol-4-yl)1,2-dihexadecanoyl-*sn*-glycero-3-phosphoethanolamine, triethylammonium salt (NBD-PE) was purchased from Molecular Probes.

**Synthesis and compound characterization:** Detailed description of synthesis protocols and compound characterization are provided in the Supporting Information.

**Construction of the expression plasmids:** N-terminal fusions of rat PKC with EGFP were generated by inserting cDNAs into the multiple cloning site of the pEGFP-N3 (Clontech Laboratories) mammalian expression vector as described previously.<sup>[14,15]</sup> The cDNA encoding PKC-ECFP was generated as described.<sup>[16]</sup>

**Cell culture and transfection:** MCF-7 cells were grown in Dulbecco's modified Eagle's medium with fetal calf serum (10%). For confocal studies the cells were plated on glass coverslips and transfected after 16–24 h with Lipofectamine-2000 (Invitrogen) by following the instructions provided by the manufacturer. The cells were examined under the microscope 16 h after transfection. Coverslips were washed with extracellular buffer HBS (3 mL; 120 mM NaCl, 25 mM glucose, 5.5 mM KCl, 1.8 mM CaCl<sub>2</sub>, 1 mM MgCl<sub>2</sub>, 20 mM HEPES, pH 7.2). All added substances were dissolved or diluted in HBS. DAG-lactones and PMA were dissolved in DMSO and diluted to the final concentration with extracellular buffer shortly before the experiment. During the experiment, the cells were not exposed to DMSO concentrations higher than 1%. All experiments were carried out at 37 °C by using a Leica CTI controller 3700 incubator. Experiments were performed independently on at least three different occasions; recordings were obtained from 10–16 cells in each experiment.

**Confocal imaging and data analysis of EGFP variants:** Cells were washed with HBS and analyzed by using a Leica TCS SP2 confocal system with a Nikon HCX-PL-APO 63x/1.4-0.6 NA oil immersion objective. During imaging, cells were stimulated with 40 μM DAG-lactones or PMA. Confocal images of EGFP constructs were obtained by excitation with a laser Ar/ArKr at 488 nm and emission was collected at wavelengths 505–550 nm. Confocal images of ECFP were obtained by excitation with a blue laser diode at 405 nm and emission was recorded at wavelengths 470–490 nm. The time series were analyzed by using the quantification profile tool included in the Leica confocal software. An individual analysis of protein translocation for each cell was performed by tracing a line intensity profile across the cell.<sup>[17]</sup> The relative increase in plasma membrane localization (*R*) of the enzyme for each time point was calculated by using the ratio  $R = (I_{mb} - I_{cyt}) / I_{mb}$ , where *I*<sub>mb</sub> is the fluorescence intensity at the plasma membrane and *I*<sub>cyt</sub> is the average cytosolic fluorescence intensity. The *R*<sub>max</sub> is the maximal relative increase in plasma membrane localization of the enzyme and *t*<sub>1/2</sub> is the half-time of translocation. Both parameters were calculated as described previously.<sup>[18]</sup> Mean values are given ± standard error deviation (SEM).

**K<sub>i</sub> measurements:** Binding of DAG-lactones to PKC was determined by competition of [20-<sup>3</sup>H]phorbol 12,13-dibutyrate (PDBu) binding as described previously.<sup>[19]</sup> The assays were carried out at 37 °C in the presence of phosphatidylserine (100 μg mL<sup>-1</sup>). Values represent the mean ± SEM of triplicate independent assays, with complete dose response curves determined in each assay.

**Fluorescence quenching:** NBD-PE was added to the DMPC vesicles at a molar ratio of 1:100 (probe/total phospholipids) and the lipids were then dried together in vacuo prior to sonication. Samples were prepared by mixing a selected quantity of DAG-lactones with the vesicles (30 μL) containing the fluorescent probe and Tris base buffer (30 μL; 50 mM, pH 8.2) followed by addition of distilled water (total volume 1.5 mL). The quenching reaction was initiated by adding sodium dithionite from a stock solution (0.6 M in 50 mM

Tris base buffer, pH 11) to give a final concentration of 1 mM. The decrease in fluorescence emission was recorded for 5 min at room temperature by using 469 nm excitation and 560 nm emission on an Edinburgh Co. FL920 spectrofluorimeter (Edinburgh Instruments, UK). The fluorescence decay curves were calculated as a percentage of the initial fluorescence measured before the addition of dithionite.

**Differential scanning calorimetry:** The multilamellar dispersion was achieved by dissolving DMPC in chloroform/ethanol (1:1) and drying in vacuo to constant weight. This was followed by addition of deionized water (final concentration 2 mM). Glass beads were then added and the sample shaken. DSC experiments were performed on a VP-DSC calorimeter (MicroCal, USA). Distilled water served as a blank. Selected quantities of DAG-lactones were added and heating scans were run at a rate of 1 °C min<sup>-1</sup>. Data analysis was performed by using Microcal Origin 6.0 software.

## Acknowledgements

This research was supported in part by the Intramural Research Program of the National Institutes of Health, Center for Cancer Research, National Cancer Institute. Grants from the Fundación Médica Mutua Madrileña-Spain, Fundación Séneca Spain 08700/PI/08 and MICINN-Dirección General de Investigación Spain (BFU2008-01010).

**Keywords:** diacylglycerol (DAG)-lactones · membrane anchoring · membranes · protein kinases · vesicles

- [1] S. G. Rhee, *Annu. Rev. Biochem.* **2001**, *70*, 281–312.
- [2] E. M. Griner, M. G. Kazanietz, *Nat. Rev. Cancer* **2007**, *7*, 281–294.
- [3] Y. Nishizuka, *Science* **1992**, *258*, 607–614.
- [4] H. J. Mackay, C. J. Twelves, *Nat. Rev. Cancer* **2007**, *7*, 554–562.
- [5] S. H. Choi, T. Hyman, P. M. Blumberg, *Cancer Res.* **2006**, *66*, 7261–7269.
- [6] V. E. Marquez, P. M. Blumberg, *Acc. Chem. Res.* **2003**, *36*, 434–443.
- [7] J. H. Kang, S. Benzaria, D. M. Sigano, N. E. Lewin, Y. Pu, M. L. Peach, P. M. Blumberg, V. E. Marquez, *J. Med. Chem.* **2006**, *49*, 3185–3203.
- [8] M. J. Rashkin, R. M. Hughes, N. T. Calloway, M. L. Waters, *J. Am. Chem. Soc.* **2004**, *126*, 13320–13325.
- [9] J. C. McIntyre, R. G. Sleight, *Biochemistry* **1991**, *30*, 11819–11827.
- [10] R. B. Gennis, *Biomembranes: Molecular Structure and Function*, Springer, New York, **1989**.
- [11] O. G. Mouritsen, *Chem. Phys. Lipids* **1991**, *57*, 179–194.
- [12] L. Philosof-Mazor, R. Volinsky, M. J. Comin, N. E. Lewin, N. Kedei, P. M. Blumberg, V. E. Marquez, R. Jelinek, *Langmuir* **2008**, *24*, 11043–11052.
- [13] O. Raifman, S. Kolusheva, M. J. Comin, N. Kedei, N. E. Lewin, P. M. Blumberg, V. E. Marquez, R. Jelinek, *FEBS J.* **2010**, *277*, 233–243.
- [14] M. Jose Lopez-Andreo, J. C. Gomez-Fernandez, S. Corbalan-García, *Mol. Biol. Cell* **2003**, *14*, 4885–4895.
- [15] C. Marin-Vicente, J. C. Gomez-Fernandez, S. Corbalan-García, *Mol. Biol. Cell* **2005**, *16*, 2848–2861.
- [16] S. Sánchez-Bautista, S. Corbalán-García, A. Pérez-Lara, J. C. Gómez-Fernández, *Biophys. J.* **2009**, *96*, 3638–3647.
- [17] T. Meyer, E. Oancea, *Methods Enzymol.* **2000**, *327*, 500–513.
- [18] M. Guerrero-Valero, C. Ferrer-Orta, J. Querol-Audi, C. Marin-Vicente, I. Fita, J. C. Gomez-Fernandez, N. Verdaguer, S. Corbalan-García, *Proc. Natl. Acad. Sci. USA* **2009**, *106*, 6603–6607.
- [19] N. E. Lewin, P. M. Blumberg, N. J. Clifton, *Methods Mol. Biol.* **2003**, *233*, 129–156.

Received: June 11, 2010

Published online on August 16, 2010